THE JOURNAL OF PHYSICAL CHEMISTRY B

Article

pubs.acs.org/JPCB

Spectroscopic Investigation of the Effect of Salt on Binding of Tartrazine with Two Homologous Serum Albumins: Quantification by Use of the Debye–Hückel Limiting Law and Observation of Enthalpy–Entropy Compensation

Priyanka Bolel, Shubhashis Datta, Niharendu Mahapatra, and Mintu Halder*

Department of Chemistry, Indian Institute of Technology Kharagpur, Kharagpur-721302, India

Supporting Information

ABSTRACT: Formation of ion pair between charged molecule and protein can lead to interesting biochemical phenomena. We report the evolution of thermodynamics of the binding of tartrazine, a negatively charged azo colorant, and serum albumins with salt. The dye binds predominantly electrostatically in low buffer strengths; however, on increasing salt concentration, affinity decreases considerably. The calculated thermodynamic parameters in high salt indicate manifestation of nonelectrostatic interactions, namely, van der Waals force and hydrogen bonding. Site-marker competitive binding studies and docking simulations indicate that the dye binds with HSA in the warfarin site and with BSA at the interface of warfarin and ibuprofen binding sites. The docked poses indicate nearby amino acid positive side chains, which are possibly responsible for electrostatic interaction. Using the Debye–Hückel interionic attraction theory for binding equilibria, it is shown that, for electrostatic binding the calculated free energy change increases linearly with square root of ionic strength. Also UV–vis, fluorescence, CD data indicate a decrease of interaction with salt concentration. This study quantitatively relates how ionic strength modulates the strength of the protein–ligand electrostatic interaction. The binding enthalpy and entropy have been found to compensate one another. The enthalpy–entropy compensation (EEC), general property of weak intermolecular interactions, has been discussed.

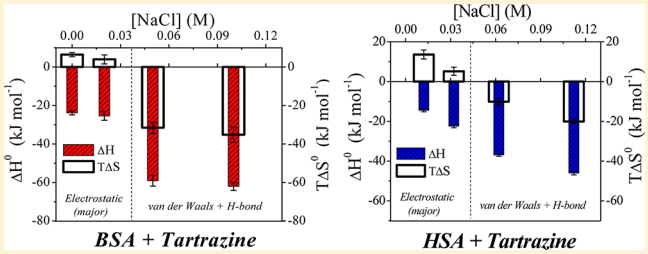

1. INTRODUCTION

The study of the binding and effects of small exogenous ligands to proteins remains one of the core aspects of research in biophysics. Among other processes, ligand binding can regulate the function of proteins including inhibition of their actions. Investigation of dyes, with different structures, binding to protein can help in the collection of new data enabling better understanding of dye–protein interaction mechanisms. Dyes have been extensively used in biological research throughout the last several decades. When examining the published literature, it is found that such studies have always been dictated by dye availability rather than designing a new one.

It is well-known that the absorption, distribution, metabolism, and excretion of various ligands are strongly affected by the protein–ligand interactions in the blood plasma.[1] Human serum albumin (HSA) is the most abundant protein in plasma, present in 6.0×10^{-4} M, contributes to about 80% of the blood osmotic pressure,[2,3] and is composed of a single chain of 585 amino acid residues. It has three homologous α-helical domains (I, II, and III), and each domain is further divided into two subdomains (A and B). SA contains two principal binding sites (i.e., Sudlow's site I and site II). These are located in the specialized cavities of subdomains IIA and IIIA, respectively, as well as some minor sites (i.e., tamoxifen and digitoxin sites).[4,5] Bovine serum albumin (BSA) is homologous, having ~88% sequence homology, with HSA and is the major soluble protein component of the blood serum of cow. Serum proteins bind a variety of ligands such as fatty acids, carboxylic acids, bilirubin, metal ions, steroids, pharmaceuticals, and several dyes.[6−12] The relative strengths of these bindings are important when the use of azo-food dyes is considered since competition between metabolites and dye molecules can interfere with the function of SA as transport proteins. Certain drugs bound by SA may also get released if the protein has stronger affinity for food dyes. This is especially evident from the binding enthalpies and entropies; although these two quantities can compensate for one another, there is often little or no net change in the overall ΔG°,[13] which is the so-called enthalpy–entropy compensation.

Characterization of the molecular basis of such interactions, from binding constant, thermodynamics, and binding site, is essential for understanding various processes in biological systems. In this regard, it is important to explore if such interactions can be externally perturbed by changing the environmental factors like the presence of salts, etc. This is

Received: May 10, 2012
Revised: July 8, 2012
Published: July 26, 2012

dx.doi.org/10.1021/jp304537m | J. Phys. Chem. B 2012, 116, 10195–10204

because salts are a very essential component for living systems, and interactions of electrostatic origin should be affected with added salt but, to nonelectrostatic interactions, salts will just behave as inert. Under physiological conditions of isotonic environment (equivalent to 0.9% NaCl), interaction of many small molecules with proteins may get suppressed if it had a lion's share of electrostatic interaction. Since, in electrostatic interaction, there is formation of an ion pair between oppositely charged partners, chemically inert salts (electrolyte) will shield these interacting charges, which tend to reduce the extent of ion pair formation. That is, with increase of added salt concentration, the manifestation of electrostatic forces progressively reduces, and ultimately at some higher salt concentration, the residual affinity should remain due to interactions of other origins only.

So on this ground, we can expect the thermodynamics of ligand binding to show an evolution from electrostatic to other modes as salt concentration is increased. The magnitude of thermodynamic parameters will alter accordingly.

Moreover, the affinity of binding between the ligand and the plasma protein can supply vital information on the pharmacological and toxicological actions, biotransformation, biodistribution, etc., of ligands since it has been demonstrated that the distribution and free concentration of various ligands can be drastically changed as a result of their binding to SAs.[14,15] Consequently, the study on the interaction of ligand with serum albumin is of imperative and fundamental importance.

When considering SAs and charged azo-dyes, especially negatively charged sulfonated azo food dyes, we have very recently reported binding of cochineal red A (CR, a synthetic azo food colorant) with SAs that occurs via electrostatic interaction,[16] and the primary binding site is site-I. This has been further confirmed from salt variation studies. Several studies have also confirmed that the electrostatic attraction is significant between the negative sulfonate group and the positively charged amino acid side chains of serum albumin.[17,18] Thus, dyes with sulfonate groups are likely to attract the positively charged side chains of a protein.

In another recent report,[19] it is found that sulfonated azo food dyes predominantly bind to BSA and HSA via hydrogen bonding and van der Waals interactions. These experiments are carried out in a buffer with relatively higher salt concentration (~20 mM). We became very curious to know why such similar water-soluble food dye should bind to the same protein due to different forces. Also, the reported binding constant[19] appeared to be lower compared to our studies with cochineal red A. We thought that exploration of the strength of interaction with and without added salt using various techniques, namely, UV–vis, CD, and thermodynamic data from fluorescence, could probably answer this query.

We have made a comparative account of exploration for the binding and associated thermodynamic parameters as a function of ionic strength (added salt) for tartrazine with BSA and HSA, in buffered solution, using general optical spectroscopic techniques. This comparative study will be the first one to look into how the binding energetics is modulated with salt and what could be the possible reasons.

2. MATERIALS AND METHODS

HSA (~99%, essentially fatty acid free) is purchased from Fluka. BSA (≥98%), tartrazine (TZ, Figure 1), ibuprofen (≥98%), and warfarin are obtained from Sigma-Aldrich. All experiments are carried out in 5 mM phosphate buffer of pH 7.4. For preparing solutions of various ionic strengths, the required weighed amount of NaCl (analytical grade, Merck) has been added to 5 mM phosphate buffer, and this NaCl-containing buffer has been used to make various protein: dye compositions in salt variation studies. All solutions are prepared in ultra pure water. The pH of solutions is measured with Eutech pH 510 ion pH-meter.

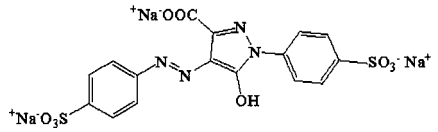

Figure 1. Molecular structure of tartrazine.

2.1. UV–Vis Absorbance Spectra. UV–vis absorbance spectra are recorded on a Shimadzu UV-1601 absorption spectrophotometer against a solvent blank reference in the wavelength range of 300–650 nm. Experiments are performed by keeping the tartrazine concentration at 20 μM.

2.2. Fluorescence Measurements. All steady-state corrected fluorescence spectra are recorded on a Jobin Yvon-Spex Fluorolog-3 spectrofluorimeter equipped with a thermostatic cell holder using a 1 cm path length quartz cuvette. Quenching experiments are performed by keeping the concentrations of HSA and BSA fixed at 4 μM and 2 μM, respectively, and quencher (TZ) concentration is varied from 0 to 12 μM. The steady-state fluorescence experiments have been carried out at 290, 300, and 310 K. An excitation wavelength of 295 nm is used in all cases for selective excitation of the tryptophan (Trp) residues of HSA and BSA, and emission spectra are recorded from 310 to 470 nm.

2.3. Circular Dichroism Spectra. Circular dichroism measurements are made on a Jasco-810 automatic recording spectropolarimeter, using a 0.1 cm path length cell. The CD spectra are recorded in the range of 190–260 nm with a scan rate of 50 nm/min and a response time of 4 s. Three scans are accumulated for each spectrum. Appropriate baseline corrections in the CD spectra are made. Spectra are recorded as ellipticity (θ) in *mdeg*. A 10 μM protein, at pH 7.4, is maintained in the experiments. Two sets of solutions are prepared by keeping the protein/TZ molar ratio of 1:0 and 1:2 in absence and in the presence of the highest studied concentration of NaCl of 0.1 M

2.4. Molecular Docking Study. The amino acid sequence corresponding to bovine serum albumin (BSA) is obtained from http://www.uniprot.org/uniprot/P02769. PDB BLAST, with this sequence as query against the protein structure, databank identified several structures of human serum albumin. The 3D structure of HSA (PDB ID: 1AO6) with chain A is used as a template structure for homology modeling using the alignment method available in Easypred3D web server.[20] The structure has been validated using PROCHECK,[21] which measures the stereochemical quality of the protein structure. The N-terminal 24 amino acid residues in the bovine sequence that did not have an equivalence in the human serum albumin template crystal structure (PDB ID: 1AO6) are not included in the model.

The structure of tartrazine is optimized by PM3 prescription using MOPAC2009.[22] Later, tartrazine is docked using AutoDock 4.2[23] into the 3D structure of BSA. AutoDock 4.2 uses the Lamarckian genetic algorithm to search for the optimum binding site of small molecules to the protein. To recognize the binding sites in serum albumins, docking is done,

and the grid sizes are set to 60, 60, and 60 along *X*-, *Y*-, and *Z*-axes with a 0.5 Å grid spacing. The Auto Docking parameters used are GA population size, 150; maximum number of energy evaluations, 250 000. During docking, a maximum of 50 conformers are considered for each molecule, and the rms (root-mean-square) cluster tolerance has been set to 2.0 Å. The grid centers at 25.027/35.491/34.328 Å and 24.366/34.571/33.095 Å are taken for BSA and HSA, respectively.

The accessible surface area (ASA) of uncomplexed protein and their docked complexes with tartrazine are calculated using Discovery Studio Visualizer 2.5 of Accelrys Software Inc. The docked conformations with the lowest binding energy are used for analysis. A probe radius of 1.4 Å is used on structures having polar hydrogen only for calculation.

2.5. Data Analysis. All data are represented as mean ± SD. Experiments are performed in triplicates. All graphical representations and statistical analyses are done using Origin.

3. RESULTS AND DISCUSSION

3.1. Steady-State Absorbance Spectra. It is found that the UV–vis spectra (Figure 2A,B) of the dye shifts to red by about 7 nm (from 427 to 434 nm) in the presence of BSA and about 4 nm (from 427 nm to 431 nm) upon binding with HSA. This is a clear indication of the ground state interaction of the dye with protein. It is interesting to note that, in the presence of NaCl (0.1 M), the dye spectra shifts very little from 427 to 428 nm. This shows that the dye–protein interaction is considerably reduced in the presence of NaCl. This is indicative of the electrostatic interaction between SA and TZ.

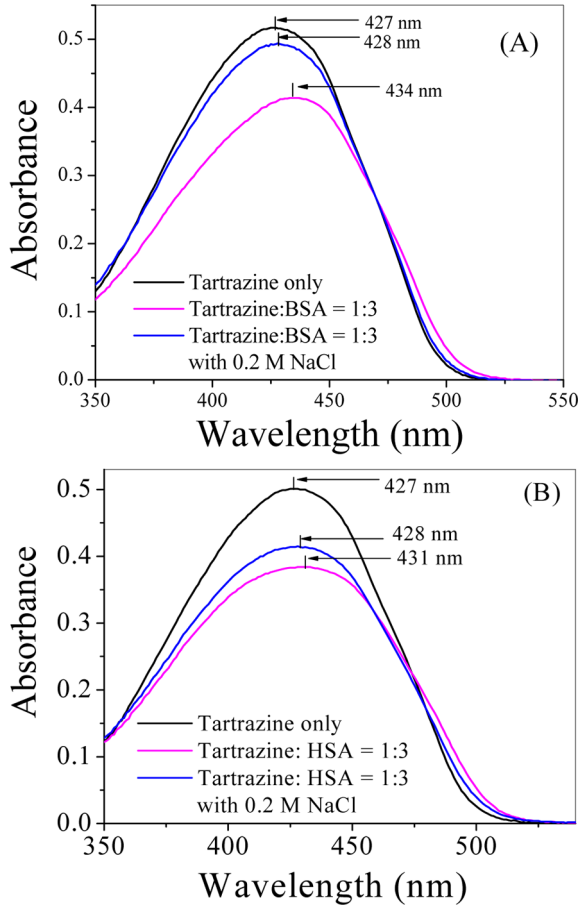

Figure 2. Absorption spectra of tartrazine at pH 7.4 in the absence and presence of (A) BSA and (B) HSA in 5 mM phosphate buffer without salt or with 0.2 M NaCl at 298 K. The concentration of tartrazine is 20 μM. The concentration of protein is varied up to 60 μM.

Tartrazine has not been found to undergo self-aggregation in the range of concentration we used, and this is confirmed by applying the Beer–Lambert law to the absorbance data. Importantly, Shahir et al.[24] have already shown that TZ does not aggregate in the concentration range used in our studies. Within this concentration range, the stoichiometry of the serum albumin–TZ complexes are determined by Job's method of continuous variation.[24,25] According to the Beer–Lambert law, if the dye and protein do not interact, the total absorbance of the mixture (A_{theo}) is equal to the sum of their individual absorbance as follows:

$$A_{theo} = \varepsilon_P C_P^0 X_P + \varepsilon_{TZ} C_{TZ}^0 X_{TZ} \quad (1)$$

where ε_P and ε_{TZ} are the molar extinction coefficients of the protein and tartrazine, respectively. $C_P^0$and C_{TZ}^0 are the concentrations of the stock solutions of the protein and dye, respectively, which are equal ($C_P^0 = C_{TZ}^0 = 1.2 \times 10^{-5}$ M). A_{exp} is the sum of absorbances of all compounds existing in solution:

$$A_{exp} = \varepsilon_P C_P + \varepsilon_{TZ} C_{TZ} + \varepsilon_C C_C \quad (2)$$

where C_P and C_{TZ} are the concentrations of protein and tartrazine in the mixture. ε_C and C_C are the molar extinction coefficient and concentration of the associate formed, respectively. By calculating A_{theo} and measuring A_{exp}, the corrected absorbance can be obtained as follows:

$$\Delta A = A_{exp} - A_{theo} \quad (3)$$

We have measured the absorbance of solutions with different mole ratios of TZ and SA at 427 nm, corresponding to dye spectra in the visible range. The corrected absorbance of particular stoichiometry (ΔA) has been plotted as function of corresponding mole fraction of the dye (X_{TZ}). For both HSA and BSA, a minimum at X_{TZ} = 0.5 has been observed (Figure 3), which corresponds to 1:1 stoichiometry of complexes.

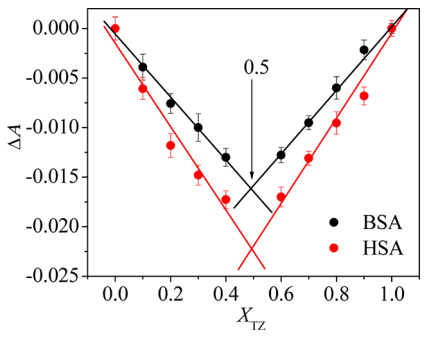

Figure 3. Job's plots for TZ–HSA and TZ–BSA in 5 mM phosphate buffer of pH 7.4 at 298 K.

There is not much shift in the spectra of TZ and protein bound TZ; it is about 4–7 nm (see Figure 2). That is, these spectra are closely overlapping, and hence, calculation of accurate association constant may not be easy. However, we have attempted the other option by monitoring the quenching of intrinsic protein fluorescence as a function of TZ concentration in calculating the association constants. Also tartrazine, a very weakly fluorescent dye with singlet quantum yield of (6.09 ± 0.06) × 10^{-5} (see Supporting Information),

dx.doi.org/10.1021/jp304537m | J. Phys. Chem. B 2012, 116, 10195–10204

does not have fluorescence overlapping with protein emission (see Figure S1 in Supporting Information).

3.2. Steady-State Fluorescence Studies. The intrinsic fluorescence intensities of tryptophan residues of HSA and BSA are found to decrease with the increase of TZ concentration and a blue shift of about 4−5 nm (Figure S2 in Supporting Information), which is an indication of the change of microenvironment of the fluorophore due to dye binding.

All fluorescence spectra are corrected for the absorption of quencher at the excitation and emission wavelengths of the fluorophore. Optical absorption of the quencher in the excitation region decreases the effective intensity of the exciting light beam, and its absorption in the emission region decreases the measured fluorescence intensity. Since the absorption increases with the increase of the quencher concentration, this induces an apparent quenching and increases the real magnitude of the quenching constants obtained from steady-state experiments. The correction factor[26] η is given by the following equation:

$$\eta = \frac{A_{x_0}A_{y_0}(1 - 10^{-A_{x_i}})(1 - 10^{-A_{y_i}})}{A_{x_i}A_{y_i}(1 - 10^{-A_{x_0}})(1 - 10^{-A_{y_0}})} \quad (4)$$

where A_{x_0}, A_{y_0} are the fluorophore absorbances, and $A_{x_i} = A_{x_0} + \Delta A_{x_i}$ and $A_{y_i} = A_{y_0} + \Delta A_{y_i}$ are total absorbances of the fluorophore and the quencher (ΔA_{x_i} and ΔA_{y_i}) at the excitation and emission wavelengths, respectively. Now the corrected fluorescence ratio F^0/F is given by

$$\frac{F^0}{F} = \left(\frac{F^0}{F}\right)_{\text{obs}} \eta \quad (5)$$

where $(F^0/F)_{\text{obs}}$ is the experimentally observed (measured) data.

Figure 4 represents typical Stern−Volmer (S−V) plots for fluorescence quenching of two homologous serum albumins,

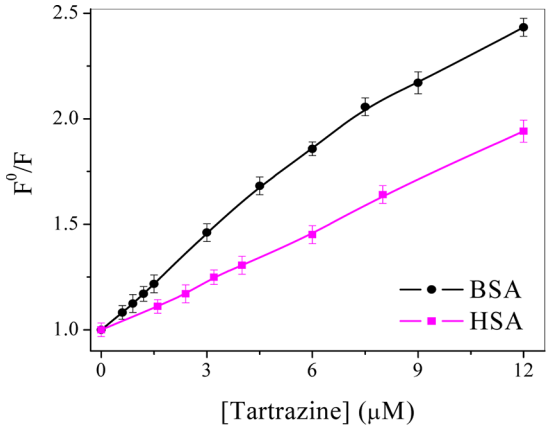

Figure 4. Representative Stern−Volmer plot for tartrazine−BSA and tartrazine−HSA systems in 5 mM phosphate buffer of pH 7.4 at 300 K. Symbols with cap include error bar.

HSA and BSA, by TZ. All the corrected S−V plots are connected by smooth lines. The data shows that, with an increase in salt concentrations, the extent of quenching decreases for both BSA and HSA (Figure 5A,B).

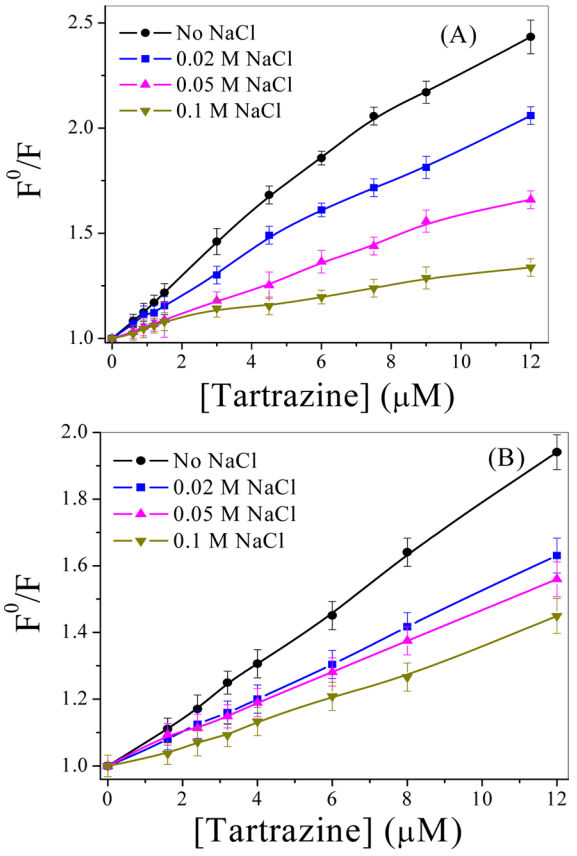

Figure 5. Quenching plot of (A) tartrazine−BSA and (B) tartrazine−HSA systems in the presence of increasing concentration of added NaCl in 5 mM phosphate buffer of pH 7.4 and 300 K. Symbols with cap include error bar.

The association (binding) constants have been calculated from the modified S−V equation[27] (eq 6) from data at different temperatures and ionic strengths.

$$\frac{F^0}{\Delta F} = \frac{1}{f_a K_\alpha}\frac{1}{[Q]} + \frac{1}{f_a} \quad (6)$$

In that case, ΔF is the difference in fluorescence intensity when measured in the absence and in presence of the quencher [Q], K_α is the effective association (quenching) constant for the accessible fluorophores, and f_a is the fraction of accessible fluorophores. The computed K_α for BSA and HSA can be found in Table 1. In both cases, the values of f_a are found to be close to unity. The decreasing trend of K_α with increasing temperature and ionic strength is observed.

The corresponding calculated thermodynamic parameters are also listed in Table 2. If we have a closer look at this table, we find a nice evolution of sign and magnitude of the numbers as a function of added salt for both proteins.

Since the extent of interaction is found to be very much dependent on the amount of electrolyte present, we have carried out experiments in a dilute buffer (without added salt) of 5 mM strength. To see the effect of salt, NaCl concentration is varied from 0 to 0.1 M by adding as solution from the outside to the respective protein−dye mixture in the buffer.

Let us consider the following binding equilibrium between the dye and protein:

$$P + D \rightleftharpoons PD$$

dx.doi.org/10.1021/jp304537m | J. Phys. Chem. B 2012, 116, 10195−10204

Table 1. Modified Stern–Volmer Association Constant (K_α) for TZ–BSA and TZ–HSA Systems at Different Concentrations of Added NaCl and Temperatures

		BSA		HSA	
NaCl (M)	temperature (K)	K_α[a]	R	K_α[a]	R
0	290	$(2.78 \pm 0.025) \times 10^5$	0.999	$(1.01 \pm 0.03) \times 10^5$	0.999
0	300	$(1.86 \pm 0.055) \times 10^5$	0.999	$(7.9 \pm 0.03) \times 10^4$	0.998
0	310	$(1.47 \pm 0.01) \times 10^5$	0.995	$(6.86 \pm 0.02) \times 10^4$	0.999
0.02	290	$(1.85 \pm 0.03) \times 10^5$	0.997	$(9.14 \pm 0.2) \times 10^4$	0.991
0.02	300	$(1.45 \pm 0.07) \times 10^5$	0.998	$(6.27 \pm 0.13) \times 10^4$	0.995
0.02	310	$(9.34 \pm 0.45) \times 10^4$	0.999	$(5.02 \pm 0.15) \times 10^4$	0.989
0.05	290	$(1.37 \pm 0.011) \times 10^5$	0.999	$(8.0 \pm 0.3) \times 10^4$	0.996
0.05	300	$(5.61 \pm 0.28) \times 10^4$	0.998	$(4.29 \pm 0.17) \times 10^4$	0.999
0.05	310	$(2.82 \pm 0.08) \times 10^4$	0.991	$(2.98 \pm 0.06) \times 10^4$	0.998
0.1	290	$(1.10 \pm 0.02) \times 10^5$	0.996	$(6.0 \pm 0.18) \times 10^4$	0.998
0.1	300	$(3.83 \pm 0.15) \times 10^4$	0.998	$(3.06 \pm 0.085) \times 10^4$	0.999
0.1	310	$(2.37 \pm 0.1) \times 10^4$	0.993	$(1.75 \pm 0.05) \times 10^4$	0.985

[a]Concentration is expressed in mol L^{-1}.

Table 2. Thermodynamic Parameters for TZ–SA System at Different Ionic Strengths

NaCl (M)	ionic strength, I (M)[a]	ΔH^0 (kJ/mol)	ΔS^0 (J/K·mol)	ΔG^0 (298 K)(kJ/mol)	ΔR
		BSA			
0	0.012	−23.87 ± 0.5	+21.7 ± 1.1	−30.34 ± 0.6	0.991
0.02	0.032	−25.45 ± 1.21	+13.36 ± 4.34	−29.43 ± 0.9	0.983
0.05	0.062	−59.13 ± 1.77	−105.78 ± 2.95	−27.61 ± 0.8	0.995
0.1	0.112	−62.05 ± 1.10	−117.99 ± 3.98	−26.89 ± 1.07	0.991
		HSA			
0	0.012	−14.49 ± 0.72	+45.69 ± 3.27	−28.10 ± 0.84	0.991
0.02	0.032	−22.45 ± 0.81	+17.38 ± 2.03	−27.63 ± 0.83	0.992
0.05	0.062	−36.99 ± 0.64	−34.02 ± 1.81	−26.86 ± 1.1	0.991
0.1	0.112	−46.07 ± 0.05	−67.51 ± 0.05	−25.95 ± 0.78	0.999

[a]Ionic strength of 5 mM phosphate buffer is 0.012 M.

$$K_{eq} = \frac{a_{PD}}{a_P a_D} = \frac{c_{PD}}{c_P c_D} \times \frac{\gamma_{PD}}{\gamma_P \gamma_D} = K_\alpha \times \frac{\gamma_{PD}}{\gamma_P \gamma_D}$$

where a is the activity, c is the analytical concentration, and γ is the activity coefficient of the concerned ions. Taking the logarithm of both the sides, we get

$$\ln K_{eq} = \ln K_\alpha + (\ln \gamma_{PD} - \ln \gamma_P - \ln \gamma_D)$$

or

$$-RT \ln K_{eq} = -RT \ln K_\alpha - RT(\ln \gamma_{PD} - \ln \gamma_P - \ln \gamma_D)$$

or

$$\Delta G^0_{I\to 0} = \Delta G^0 - RT(\ln \gamma_{PD} - \ln \gamma_P - \ln \gamma_D)$$

Here, K_α is the association (binding) constant, and K_{eq} is the association (binding) constant when activity coefficients are unity. It looks like that free energy change will also depend on the magnitude of the activity coefficients, which will deviate from unity in the presence of other ions. Here, ΔG^0 is the standard free energy change, and $\Delta G^0_{I\to 0}$ is the standard free energy change when activity coefficients are unity; that is at zero ionic strength. On applying Debye–Hückel limiting law,[28−30] based on interionic attraction theory, for dilute solutions, we get

$$\Delta G^0_{I\to 0} = \Delta G^0 + 2.303RTA(Z_{PD}{}^2 - Z_D{}^2 - Z_P{}^2)I^{1/2}$$

For a given dye-protein pair, the term in the parentheses (ξ, say) is constant. Its sign and magnitude will depend on the difference between the square of charges of the species under equilibrium. Also for water, at 298 K, $A = 0.509$. Thus,

$$\Delta G^0_{I\to 0} = \Delta G^0 + 2904.28\xi I^{1/2} \quad (7)$$

or

$$\Delta G^0 = \Delta G^0_{I\to 0} - 2904.28\xi I^{1/2} \quad (8)$$

A positive slope of ΔG^0 vs $I^{1/2}$ plot corresponds to a negative value of ξ. Also, the intercept corresponds to the magnitude of free energy change at zero ionic strength. Nice linear plots indicate applicability of the Debye–Hückel limiting law to SA–TZ interaction. We find that the plot has positive slope, which indicates that ξ has a negative value (Figure 6) for both BSA and HSA. Since ionic strength variation clearly indicates electrostatic interaction and affinity is found to reduce with salt concentrations, it should be a case of binding of negatively charged TZ in the positively charged part (pocket) of SA. Actually, $\xi = (Z_P + Z_D)^2 - Z_P{}^2 + Z_D{}^2 = 2Z_PZ_D$, Z_D = negative for TZ, and Z_P must be some positive value. Thus, ξ is negative, which indicates the same conclusion.

Here, it should be noted that both HSA and BSA have a net charge of −18 at pH 7.4.[31,32] Hence, the binding interaction of negative dye TZ[33] and these serum albumins is expected to be somewhat weaker due to columbic repulsion. Since these two proteins are having sequence homology; we may expect them to have comparable binding affinities with TZ as the dye binds in the similar subdomains in both cases (see Tables 1 and 2, and discussion relating to competitive binding later on). As

dx.doi.org/10.1021/jp304537m | J. Phys. Chem. B 2012, 116, 10195−10204

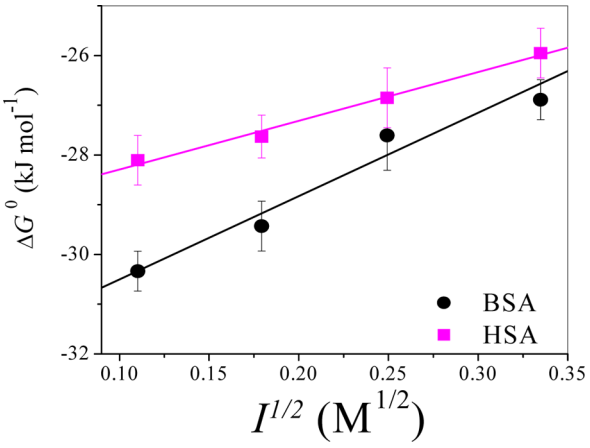

Figure 6. Plot of ΔG^0 vs $I^{1/2}$ for both TZ–BSA and TZ–HSA systems at 298 K.

pointed out earlier that the dye–protein interaction is predominantly electrostatic in origin, one may expect that local charge of binding site should be more important than the overall charge of the protein because the binding is confined at a specific location (pocket). Hence, by neglecting the size and overall charge of a protein molecule, we can apply the Debye–Hückel interionic attraction theory to test its applicability. So, we have attempted Debye–Hückel limiting law to the thermodynamic numbers (ΔG^0) for different ionic strengths (using eq 8). Similar application of Debye–Hückel limiting law is found to explain the electrostatic effects in the folding of a single domain protein FynSH3.[34]

From the above plot (Figure 6), we find that ΔG^0 increases, and hence, affinity reduces with an increase of salt added. This is a clear indication of predominance of electrostatic force for TZ–BSA and TZ–HSA interactions in dilute buffer at pH7.4. At and above 0.05 M NaCl, the sign and magnitude of thermodynamic parameters further indicate predominance of nonelectrostatic interaction over electrostatic contributions. So, according to interionic attraction theory,[28−30] when added salt increases in concentration, it tends to reduce ionic attractions, and hence, manifestation of electrostatic interaction fades out. This is also found to be the case when we recorded CD spectra in the absence and in the presence of 0.1 M NaCl (see the next section). Similar conclusion can be had from the absorbance measurements without and with NaCl (Figures 2A,B). Since the intercept of the ΔG^0 vs $I^{1/2}$ plot corresponds to the standard free energy change at zero ionic strength, it is the true free energy change ($\Delta G^0_{I\to 0}$), not perturbed by ionic atmosphere. $\Delta G^0_{I\to 0}$ = −29.27 ± 0.11 kJ/mol for HSA, and −32.11 ± 0.39 kJ/mol for BSA are found from the intercept. Thus, salt variation can furnish the actual binding strength.

3.3. Circular Dichroism Study. Circular dichroism spectroscopy is very sensitive in monitoring the secondary structural change of protein upon ligand binding.[35] The CD spectra of BSA and HSA in the absence and presence of CR at two concentrations of added NaCl are shown in (Figure 7A,B). It exhibits two negative bands at 208 and 222 nm in the UV region, characteristic of typical α-helix structure.[36] These negative peaks at 208 and 222 nm both contribute to the $n \to \pi^*$ transition for the peptide bond in α-helix.[37] The CD spectra of proteins in the presence and absence of CR are similar in shape, indicating a predominantly α-helical[38] structure after dye association. Calculations are made in

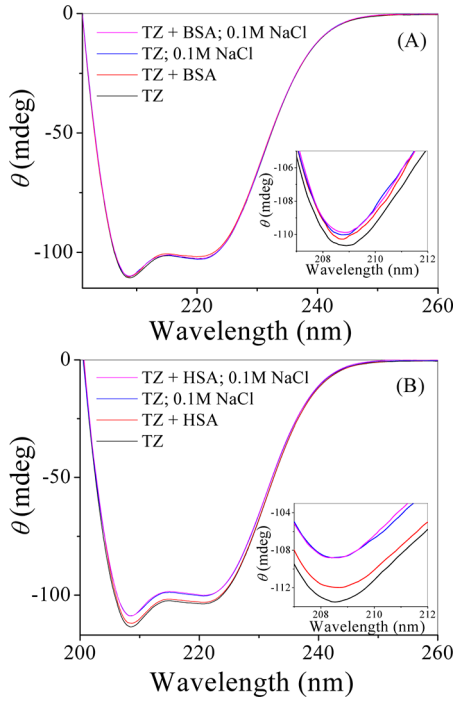

Figure 7. CD spectra of free (A) BSA and (B) HSA and that complexed with tartrazine ([protein]/[dye] = 1:2) in 5 mM phosphate buffer of pH 7.4 in the absence of salt and in the presence of 0.1 M NaCl at 298 K. Insets show the corresponding expanded wavelength region of CD spectra.

terms of mean residue ellipticity (*MRE*) in deg cm^2 dmol^{-1} according to following equation:[39]

$$MRE = \frac{\theta_{obs}(\text{mdeg})}{10 n_r l c_p} \tag{9}$$

where θ_{obs} is the observed ellipticity in milldegrees at 208 nm, n_r is the number of amino acid residues, l is the path length of the cell, and c_p is the molar concentration of the protein. The % α-helix content is then obtained from the *MRE* values at 208 nm using the following equation:[40]

$$\alpha\text{-helix}(\%) = \left\{\frac{(-MRE_{208} - 4000)}{33000 - 4000}\right\} \times 100 \tag{10}$$

where MRE_{208} is the experimental *MRE* value of proteins at 208 nm, 4000 is the *MRE* value of the β form and random coil conformation at 208 nm, and 33 000 is the *MRE* value of a pure α-helix at 208 nm. The values of n_r are taken as 583 and 585 for BSA and HSA, respectively.[41]

The obtained values of % α-helix for both the proteins in pH 7.4 at two different added NaCl are summarized in Table 3. The observed α-helix contents of uncomplexed BSA and HSA

Table 3. α-Helix (%) Content of Free and Complexed Serum Albumins with Tartrazine in the Absence and in the Presence of NaCl in 5 mM Phosphate Buffer of pH 7.4 at 298 K; Concentration of Serum Albumin Is 10 μM

	no salt (α-helix (%))		0.1 M NaCl (α-helix (%))	
tartrazine (μM)	BSA	HSA	BSA	HSA
0	51.1	52.81	50.72	50.09
20	50.76	51.99	50.67	50.1

dx.doi.org/10.1021/jp304537m | J. Phys. Chem. B 2012, 116, 10195−10204

are of 51.1% and 52.81% for no added NaCl and 50.72% and 50.09% for 0.1 M NaCl cases, respectively. The decrease in α-helical content is more upon binding of TZ in the absence of added NaCl compared to that in its presence. This means that, in the presence of salt, interaction between protein and TZ is considerably reduced.

3.4. Competitive Binding with Warfarin and Ibuprofen. Competitive binding with warfarin indicates that TZ binds with both SAs in site-I (subdomain-IIA). Moreover, with BSA, we find that ibuprofen does also compete with TZ binding (Figure 8). For HSA, ibuprofen does not seem to compete with

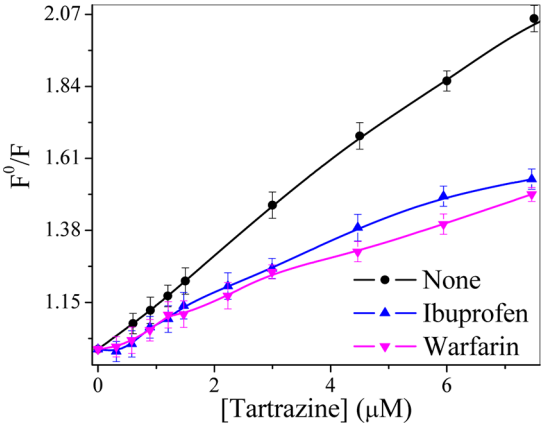

Figure 8. Effect of selected site-markers on tartrazine–BSA in 5 mM phosphate buffer of pH 7.4 at 298 K. [BSA] = 1.5 μM and [protein]/[site-marker] = 1:1. Symbols with cap include error bar.

TZ (see Figure S3 of Supporting Information). The binding constants (K_b) are determined by the following equation, where n is number of binding sites:

$$\log\left(\frac{F^0 - F}{F}\right) = \log K_b + n \log[Q] \tag{11}$$

The binding constants are presented in Table 4, and we also find that the number of binding sites is unity, which matches that reported by Pan et al.,[19] and our stoichiometry determination, using Job's method, also indicates a 1:1 complex for both proteins. Thus, for BSA, possibly, the dye is at the interface of warfarin and ibuprofen sites, and for HSA, it is in the warfarin binding site. We will substantiate this result from molecular docking simulations and calculation of accessible surface area.

3.5. Enthalpy–Entropy Compensation (EEC). The generality of this phenomenon have been a subject of debate for many years. Although such compensation is not a thermodynamic requirement,[42,43] this has been very often observed in protein–ligand interactions.[44] In brief, stronger and more directed interactions are entropically less favorable since the tight binding constricts local motions of ligand. The enthalpic and entropic contributions are related. An increase in enthalpy by tighter binding may directly affect the entropy by restricting the mobility of the ligand molecules.[45] The detailed mechanism of enthalpy–entropy compensation is, however, system-dependent.

Figure 9 shows the ΔH^0 vs $T\Delta S^0$ plot at 298 K for BSA and HSA. A linear correlation indicates enthalpy–entropy compensation occurring in the case of binding of TZ with SA. This means that change in enthalpy is compensated by a corresponding change in the entropic term.

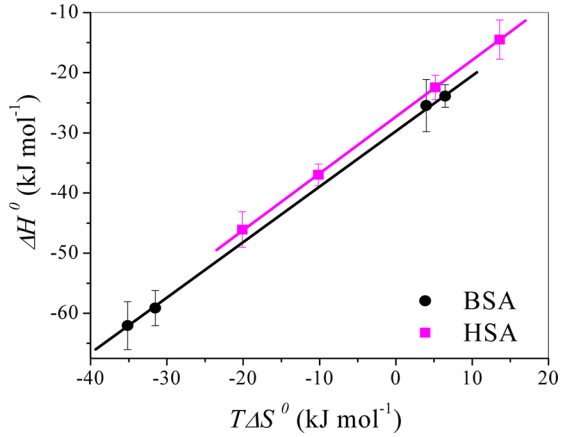

Figure 9. Plot of ΔH^0 vs $T\Delta S^0$ for both TZ–BSA and TZ–HSA systems at 298 K.

The slope of the plot for BSA (black line) is 0.92 and, for HSA, (magenta line) is 0.94, which are close to unity as expected. If we have a closer look at the thermodynamic data (Table 2), we see that up to 0.02 M NaCl, entropic contribution is positive for both BSA and HSA, but above 0.02 M, it is negative. Also, the exothermic enthalpy term increases with salt concentration. This means up to 0.02 M NaCl, the interaction is predominantly guided by electrostatic interaction and above it is hydrogen bonding and van der Waals interaction.[46] It seems reasonable to assume that, when electrostatic interaction takes predominance, the ligand part in the ion pair should not have much restriction on its local mobility (because it is a through space charge attraction, no real bond formation) as is evident from lower enthalpy and positive entropy. But above 0.02 M NaCl, hydrogen bonding and van der Waals interactions are prominent, which perhaps constricts local motion and brings in tighter binding, as evident from the calculated higher enthalpy and negative entropy.

Influence of solvent on binding can be favorable or unfavorable and enthalpy- or entropy-driven, respectively.

Table 4. Binding Constants (K_b) Obtained at 298 K from Site-Marker Competitive Binding Experiments for TZ–BSA and TZ–HSA Systems at pH 7.4

	K_b[a]			
site-marker	BSA	n	HSA	n
none	$(3.16 \pm 0.12) \times 10^5$	1.09 ± 0.05	$(2.08 \pm 0.08) \times 10^5$	1.04 ± 0.05
ibuprofen	$(5.79 \pm 0.17) \times 10^4$	0.97 ± 0.05	$(2.09 \pm 0.07) \times 10^5$	1.04 ± 0.05
warfarin	$(2.87 \pm 0.10) \times 10^4$	0.93 ± 0.04	$(1.65 \pm 0.06) \times 10^5$	1.05 ± 0.05

[a]Concentration is expressed in mol L^{-1}.

dx.doi.org/10.1021/jp304537m | J. Phys. Chem. B 2012, 116, 10195–10204

Bound water molecules can be freed upon ligand binding or, upon the other way, bind tighter impeding the incoming ligand.[47−49] Presence of bound water can result in a more rigid protein structure[50] or may be more flexible.[51] Finally, ligand binding sites in proteins can be highly solvated prior to binding or lesser solvated.[52,53] The important feature that could exist is the contribution of the solvation to the thermodynamics of ligand binding, which can be significant. Also, ligand local motion may disrupt some nearby solvent structures resulting in the increase of entropy (electrostatic interaction) and constricted local motion (hydrogen bond and van der Waals interaction) may act in reverse fashion. It appears that the interplay between electrostatic and nonelectrostatic contributions could be the key factor for the observed EEC.

Actually, entropy−enthalpy compensation (EEC) is a logical concept. Consider designing of a ligand for a protein and modulating the binding affinity by adding hydrophobic groups, H-bonding groups, or salt from outside, the last option seems to reduce the electrostatic contribution as happened in our study. Noncovalent electrostatic interactions can be operative at distance more than a hydrogen bond, which perhaps leaves some options for the ligand to wiggle. In the presence of salt, the ionic atmosphere shields electrostatic forces, and then, the mode that is responsible for binding is due to nonelectrostatic forces. Thus, the ligand will tend to bind tighter in order to increase van der Waals contacts as well as the H-bonding. The term "tighter" implies the loss of entropy. Thus, the gain in enthalpy of binding is offset by a loss in entropy. So even if the ligand is modified, the resulting free energy of binding may be very small or at least will stay almost constant because of these two opposing quantities.

It may be noted that we have attempted both steady-state and time-resolved anisotropy experiments to clarify the alterations of local motions of the dye molecules due to the addition of salt, but unfortunately, the singlet quantum yield of TZ in buffer is too low $[(6.09 \pm 0.06) \times 10^{-5}]$ to detect any light after a polarizer−analyzer pair. However, we have attempted to find out the stoichiometry of the protein−dye complex in the presence of 0.1 M salt employing Job's method,[24,25] and the stoichiometry has been found to decreases significantly from 1:1 to ∼1:0.5 (protein:TZ) for HSA and BSA indicating lesser association (see Figure S4 in the Supporting Information). This means that protein pocket should be less perturbed in the presence of salt.

Thus, the enthalpy−entropy compensation (EEC) seems widespread among ligand−protein systems. It appears universal that binding restricts motions, while motions oppose tight confinement. This behavior has been proposed to result from the reorganization of solvent (water), which contributes significantly to the enthalpy and entropy changes but not much to the change of free energy in ligand-protein binding. In the present study also, we have not observed much change in the standard free energy change with ionic strength (Table 2).

3.6. Molecular Docking Simulations. Docking of the ligand with macromolecules provides insight into the preferred binding location and can be exploited to corroborate experimental observations to a large extent. TZ has been docked into the 3D structure of BSA and HSA using AutoDock Tools.[23] These models provide the most probable binding sites and poses in the protein that have not resulted in structural alteration of the macromolecule. The principal ligand binding sites in HSA indicate that they are located in hydrophobic cavities of subdomains IIA and IIIA. Our model of BSA, obtained from homology with HSA, shows that these domains are identical to those in HSA, and the binding sites analyzed here have an equivalent binding site in HSA. From the competitive site-marker binding experiment, we have indications that TZ binds in the warfarin site of HSA, and in BSA, the possible location is at the interface of the warfarin and ibuprofen binding sites. Keeping these in mind, we have performed the docking simulations. From the lowest energy poses of docked TZ in HSA and BSA, it is clear that the location of the dye in HSA is in the warfarin binding site (site-I, subdomain IIA), and that in BSA is perfectly at the interface of two sites (namely, subdomains IIA and IIIA). The docked poses are shown in Figure 10. This is also evident from the calculation of solvent accessible surface areas of residues of the concerned domains (Tables S1 and S2 in Supporting Information) of BSA and HSA.

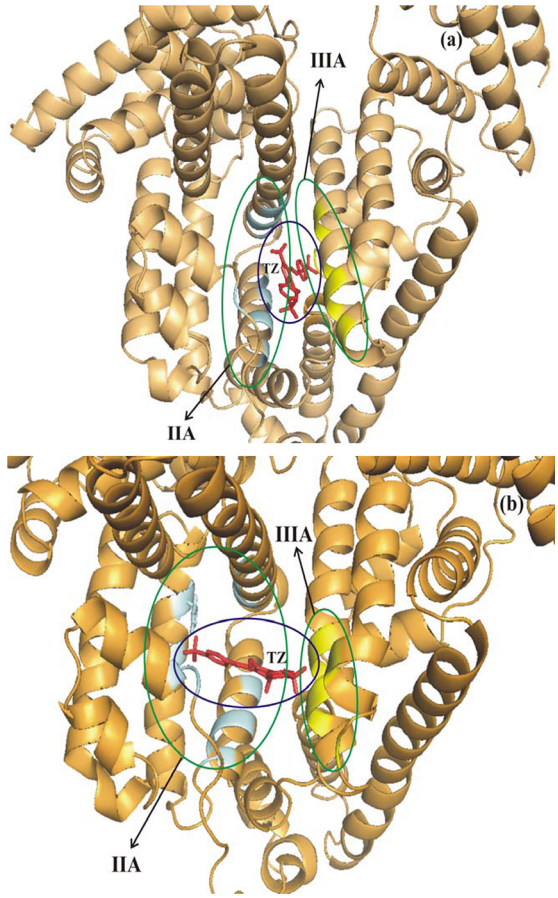

Figure 10. Docked pose of tartrazine in (a) BSA and (b) HSA.

If we look into the number of residues that have suffered from change (reduction) in ASA due to the docking of dye, we find that ten residues of subdomain IIA of HSA are involved compared to six residues of subdomain IIIA. Whereas, for BSA, eight residues of subdomain IIA are involved with nine residues of subdomain IIIA. That is, for HSA, a lesser number of amino acid residues of subdomain IIIA have reduction in ASA. Thus, for BSA, the dye possibly finds a place, wherefrom it can access both subdomains IIA and IIIA at the interface (Figure 10a), and TZ docks primarily in subdomain IIA of HSA (Figure 10b). This clearly corroborates with competitive binding results that only warfarin competes with TZ in HSA but both warfarin and

ibuprofen competes with TZ binding in case of BSA. It is important to note that, for both BSA and HSA, we find that the docked dye has nearby positively charged amino acid side chains (see Tables S1 and S2 in Supporting Information), e.g., arginine (Arg), lysine (Lys), and histidine (His), which attract the negatively charged dye due to electrostatic forces (Figure 10).

4. CONCLUSIONS

The present study provides a very important insight on to the thermodynamics of ligand−protein interaction with particular reference to electrostatic interaction. Results from UV−vis and CD spectral studies and fluorescence measurements show that ionic strength can indeed modulate the nature of interaction, and in lower ionic strengths, signatures of electrostatic interaction can be observed; however, an increase of ionic strength will overshadow electrostatic contribution and manifest other modes of interactions. Actually, the contribution of electrostatic component is much more than other modes of interaction, which perhaps masks manifestation of the non-electrostatic interactions in low or zero ionic strength. Thus, salt variation studies on binding affinity helps to establish or rule out electrostatic contribution. We have shown the applicability of this concept with tartrazine−BSA/HSA cases as examples.

The site-marker competitive binding experiments indicate that TZ binds to the warfarin binding site of HSA, and for BSA, the dye should be common to warfarin and ibuprofen binding sites, which is quite unique, although, in both cases, the binding stoichiometry is found to be 1:1. The molecular docking simulations and calculation of accessible surface area indicates the same trend.

A good enthalpy−entropy compensation (EEC) is observed with ionic strengths, and examination of the trend of variation of thermodynamic parameters indicates higher binding affinity with possibility of local motion of the ligand in lower ionic strength, and as ionic strength is increased, binding affinity is reduced with a possible tight packing of ligand with reduced mobility. Thus, variation of ionic strengths results in the internal compensation of entropy and enthalpy with some reduction in the affinity, which is evident from the lower change in the overall free energy of interaction.

As an implication of the method, we can find out the affinity at any ionic strength if we know the ΔG^0 vs $I^{1/2}$ plot for any electrostatic protein−ligand interaction. So, binding affinity can be nicely modulated externally to such a low value by adding salt such that toxic effects of these azo food dyes can, in principle, be eliminated. This will perhaps be very important to protein−dye chromatography.

At a sufficiently high ionic strength, when practically no electrostatic force can be effective between the protein and dye, the binding constant should correspond to nonelectrostatic contributions, provided salt concentration is not too high to disrupt the three-dimensional protein structures and may be close to isotonic solution. So by employing the salt variation technique, we can assess the contributions of various factors to exogenous ligand binding.

The expression based on the Debye−Hückel theory nicely correlates the free energy of binding with ionic strength, and a smaller variation of free energy with salt perhaps makes these systems showing EEC since it is a general property of weak intermolecular interactions. It is also important to note that we have perturbed the protein−ligand system in a more simpler way by altering one parameter, ionic strength, specific to electrostatic forces rather than changing a parameter that acts in a multi dimensional way; this perhaps enabled us to observe EEC. Enthalpy−entropy compensation reflects the flexibility of the surrounding structure. Clearly, EEC is an important concept in rational ligand and drug design. Also from the above studies on ionic strength variations, it is clear that, by playing with the amount of salt added, one can have control over easy reparability of charged food dyes in affinity chromatography. Finally, this salt variation approach can be a smarter tool in looking into the possible importance of electrostatic interaction in any ligand protein interaction. This study demonstrates the applicability of the Debye−Hückel theory in biomolecular ion pair formation and has the promise of a wide applicability in similar systems.

■ ASSOCIATED CONTENT

Supporting Information

Quantum yield and solubility data of tartrazine; normalized fluorescence spectra of BSA and tartrazine in 5 mM phosphate buffer of pH 7.4 at 298 K; fluorescence spectra of SA as a function of tartrazine concentration in 5 mM phosphate buffer at pH7.4; effect of selected site-markers on tartrazine−HSA in 5 mM phosphate buffer of pH 7.4 at 298 K; Job's plots of tartrazine−HSA/BSA systems in 5 mM phosphate buffer of pH 7.4 in presence of 0.1 M NaCl at 298 K; accessible surface area (ASA) in Å^2 of interacting residues of BSA (uncomplexed) and in their complex with tartrazine; accessible surface area (ASA) in Å^2 of interacting residues of HSA (uncomplexed) and in their complex with tartrazine This material is available free of charge via the Internet at http://pubs.acs.org.

■ AUTHOR INFORMATION

Corresponding Author

*Tel: +91-3222-293314. Fax: +91-3222-282252. E-mail: mintu@chem.iitkgp.ernet.in.

Notes

The authors declare no competing financial interest.

■ ACKNOWLEDGMENTS

We thank DST-India (Fund no. SR/FTP/CS-97/2006), CSIR-India (Fund no. 01/(2177)/07 EMR-II, dated 24/10/2007), and IIT-Kharagpur (ISIRD-EEM grant) for financial support. P.B. thanks UGC-India for a fellowship, N.M. thanks CSIR for fellowship, and S.D. thanks IIT-Kharagpur for fellowship. We would like to thank the anonymous reviewers for their critical comments and suggestions.

■ REFERENCES

(1) Brunmark, P.; Harriman, S.; Skipper, P. L.; Wishnok, J. S.; Amin, S.; Tannenbaum, S. R. *Chem. Res. Toxicol.* **1997**, *10*, 880−886.
(2) He, X. M.; Carter, D. C. *Nature* **1992**, *358*, 209−215.
(3) Peters, T., Jr. *All About Albumin: Biochemistry, Genetics, and Medical Applications*; Academic Press: San Diego, CA, 1995.
(4) Sudlow, G.; Birkett, D. J.; Wade, D. N. *Mol. Pharmacol.* **1975**, *11*, 824−832.
(5) Sengupta, A.; Hage, D. S. *Anal. Chem.* **1999**, *71*, 3821−3827.
(6) Kamal, J. K. A.; Zhao, L.; Zewail, A. H. *Proc. Natl. Acad. Sci. U.S.A.* **2004**, *101*, 13411−13416.
(7) Roche, M.; Dufour, C.; Loonis, M.; Reist, M.; Carrupt, P.-A.; Dangles, O. *Biochim. Biophys. Acta* **2009**, *1790*, 240−248.
(8) Bischel, H. N.; MacManus-Spencer, L. A.; Luthy, R. G. *Environ. Sci. Technol.* **2010**, *44*, 5263−5269.

(9) Hebert, P. C.; MacManus-Spencer, L. A. *Anal. Chem. Phys. Lett.* **2010**, *82*, 6463−6471.
(10) Chen, R. F. *Arch. Biochem. Biophys.* **1967**, *120*, 609−620.
(11) Peters, T.; Taniuchi, H.; Anfinsen, C. B. *J. Biol. Chem.* **1973**, *248*, 2447−2451.
(12) Klotz, I. M.; Burkhard, R. K.; Urquhart, J. M. *J. Phys. Chem.* **1952**, *56*, 77−85.
(13) Janssen, L. H. M.; Droge, J. H. M.; Durlinger, F. J. *Thermochim. Acta* **1990**, *172*, 197−202.
(14) MacManus-Spencer, L. A.; Tse, M. L.; Hebert, P. C.; Bischel, H. N.; Luthy, R. G. *Anal. Chem.* **2010**, *82*, 974−981.
(15) Monti, S.; Manet, I.; Manoli, F.; Marconi, G. *Phys. Chem. Chem. Phys.* **2008**, *10*, 6597−6606.
(16) Bolel, P.; Mahapatra, N.; Halder, M. *J. Agric. Food. Chem.* **2012**, *60*, 3727−3734.
(17) Patel, A. B.; Srivastava, S.; Phadke, R. S. *J. Biol. Chem.* **1999**, *274*, 21755−21762.
(18) Sereikaite, J. B.; Bumelis, V. A. *Cent. Eur. J. Chem.* **2008**, *6*, 509−512.
(19) Pan, X. R.; Qin, P. F.; Liu, R. T.; Wang, J. *J. Agric. Food. Chem.* **2011**, *59*, 6650−6656.
(20) Lambert, C.; Leonard, N.; Bolle, X. D.; Depiereux, E. *Bioinformatics* **2002**, *18*, 1250−1256.
(21) Laskowski, R. A.; Macarthur, M. W.; Moss, D. S.; Thornton, J. M. *J. Appl. Crystallogr.* **1993**, *26*, 283−291.
(22) Stewart, J. J. P. Stewart Computational Chemistry: Colorado Springs, CO, 2008.
(23) Morris, G. M.; Goodsell, D. S.; Halliday, R. S.; Huey, R.; Hart, W. E.; Belew, R. K.; Olson, A. J. *J. Comput. Chem.* **1998**, *19*, 1639−1662.
(24) Shahir, A. A.; Javadian, S.; Razavizadeh, B. B. M.; Gharibi, H. *J. Phys. Chem. B* **2011**, *115*, 14435−14444.
(25) Forte-Tavcer, P. *Dyes Pigm.* **2004**, *63*, 181−189.
(26) Borissevitch, I. E. *J. Lumin.* **1999**, *81*, 219−224.
(27) Lakowicz, J. R. *Principles of Fluorescence Spectroscopy*, 3rd ed.; Springer: New York, 2006.
(28) Debye, P.; Pauling, L. *J. Am. Chem. Soc.* **1925**, *47*, 2129−2134.
(29) Falkenhagen, H. *Rev. Mod. Phys.* **1931**, *3*, 412−426.
(30) Debye, P.; Hückel, E. *Phys. Z.* **1923**, *24*, 185−206.
(31) Lee, S. C.; Yeo, Y.; Park, K. *Scaffolding In Tissue Engineering*; Ma, P. X., Elisseeff, J., Eds.; CRC Press: Boca Raton, FL, 2005; pp 283−299.
(32) Yokouchi, Y.; Tsunoda, T.; Imura, T.; Yamauchi, H.; Yokoyama, S.; Sakai, H.; Abe, M. *Colloid Surf., B* **2001**, *20*, 95−103.
(33) Minioti, K. S.; Sakellariou, C. F.; Thomaidis, N. S. *Anal. Chim. Acta* **2007**, *583*, 103−110.
(34) Rios, M. A. D.; Plaxco, K. W. *Biochemistry* **2005**, *44*, 1243−1250.
(35) Haq, S. K.; Khan, R. H. *Int. J. Biol. Macromol.* **2005**, *35*, 111−116.
(36) Kamat, B. P.; Seetharamappa, J. *J. Pharm. Biomed. Anal.* **2004**, *35*, 655−664.
(37) Yang, P.; Gao, F. *The Principle of Bioinorganic Chemistry*; Science Press: Beijing, China, 2002; p 349.
(38) Hu, Y. J.; Liu, Y.; Shen, X. S.; Fang, X. Y.; Qu, S. S. *J. Mol. Struct.* **2005**, *738*, 143−147.
(39) Yuan, J. L.; Lv, Z.; Liu, Z. G.; Hu, Z.; Zou, G. L. *J. Photochem. Photobiol., A* **2007**, *191*, 104−113.
(40) Rahman, M. H.; Maruyama, T.; Okada, T.; Yamasaki, K.; Otagiri, M. *Biochem. Pharmacol.* **1993**, *46*, 1721−1731.
(41) Ni, Y.; Su, S.; Kokot, S. *Anal. Chim. Acta* **2006**, *580*, 206−215.
(42) Ford, D. M. *J. Am. Chem. Soc.* **2005**, *127*, 16167−16170.
(43) Sharp, K. *Protein Sci.* **2001**, *10*, 661−667.
(44) Whitesides, G. M.; Krishnamurthy, V. M. *Q. Rev. Biophys.* **2005**, *38*, 385−395.
(45) Dunitz, J. D. *Chem. Biol.* **1995**, *2*, 709−712.
(46) Ross, P. D.; Subramanian, S. *Biochemistry* **1981**, *20*, 3096−3102.
(47) Poornima, C. S.; Dean, P. M. *J. Comput.-Aided Mol. Des.* **1995**, *9*, 500−512.
(48) Poornima, C. S.; Dean, P. M. *J. Comput.-Aided Mol. Des.* **1995**, *9*, 513−520.
(49) Poornima, C. S.; Dean, P. M. *J. Comput.-Aided Mol. Des.* **1995**, *9*, 521−531.
(50) Mao, Y.; Ratner, M. A.; Jarrold, M. F. *J. Am. Chem. Soc.* **2000**, *122*, 2950−2951.
(51) Fischer, S.; Verma, C. S. *Proc. Natl. Acad. Sci. U.S.A.* **1999**, *96*, 9613−9615.
(52) Barratt, E.; Bronowska, A. K.; Vondrásek, J.; Cerný, J.; Bingham, R.; Phillips, S.; Homans, S. W. *J. Mol. Biol.* **2006**, *362*, 994−1003.
(53) Syme, A. *J. Palliative Care* **2010**, *26*, 212−213.